



December 5, 2024

Mary Camarata
Regional Solutions Coordinator
165 East 7th Avenue, Suite 100
Eugene, Oregon 97401

Dear Mary:

Enclosed, please find a technical memorandum (TM), prepared by Life Cycle Geo, LLC (LCG), that documents an evaluation of the transport and evolution of major ions, Biological Oxygen Demand (BOD), pH, Total Suspended Solids (TSS), and Total Dissolved Solids (TDS) in treated wastewater discharges from a proposed wastewater infiltration system in Mill City, Oregon.

The evaluation of major ions, BOD, pH, TSS, and TDS applies fate and transport in porous media fundamentals and employs the United States Geological Survey geochemical modeling code PHREEQC to simulate geochemical reactions including thermodynamic equilibrium, mineral dissolution/precipitation, ion exchange, sorption/desorption, and one-dimensional transport along the groundwater flowpath. The TM was prepared to address the Oregon Department of Environmental Quality's (DEQ's) January 16, 2024, comments on a screening-level fate and transport analysis by GSI Water Solutions, Inc. (GSI)¹. Specifically, the LCG TM addresses DEQ Comment No. 4.

LCG's modeling and assessment concludes that TSS will be attenuated during transport and effects of the infiltration system won't be observed at the Santiam River, while the geochemical parameters (e.g., BOD, pH, major ions, and TDS) can be expected to change along the flowpath to differing degrees. This conclusion, in conjunction with nitrate fate and transport modeling² and toluene/DEHP modeling³, may be used to inform the permitting framework for the proposed wastewater infiltration system.

The table on the following page summarizes the seven factors established by DEQ for evaluating functional equivalency, and how the factors are addressed by the geochemical assessment. Note that the PHREEQC model does not address Factor 1, Factor 2, Factor 3, or Factor 6. The table applies DEQ's guidance related to the U.S. Supreme Court's "functional equivalence test" in the *County of Maui v. Hawaii Wildlife Fund* decision. We make no opinion as to DEQ's guidance's consistency with that decision or related EPA guidance.

¹ GSI. 2023. Evaluation of the Environmental Fate of Residual Pollutants from an Advance (Class A) Treated Wastewater Infiltration System, Mill City, Oregon. Prepared by: GSI Water Solutions, Inc. Prepared for: Marion County. November 16.

² GSI. 2024. Evaluation of the Environmental Fate of Residual Nitrate from an Advance (Class A) Treated Wastewater Infiltration Facility, Mill City, Oregon. Prepared by: GSI Water Solutions, Inc. Prepared for: Marion County. November 26.

³ GSA. 2024. Subsurface Fate and Transport of Residual Discharges of Toluene and Di(2-ethylhexyl)phthalate from a Treated Wastewater Infiltration System, Mill City, Oregon.

Functional Equivalency Factors Addressed by the PHREEQC Model

Factor	Description	Geochemical Assessment Result ³	Factor Classification
1	Transit Time of Major Ions, TDS, pH, TSS, and BOD ¹	—	—
2	Travel Distance of Major Ions, TDS, pH, TSS, and BOD	—	—
3	Nature of Material	—	—
4	Chemical Change of Major Ions, TDS, pH, TSS, and BOD	Distinct (major ions) ² 8%-9% Reduction (TDS) Similar to Background (pH) 100% Reduction (TSS) >23% Reduction (BOD)	Varies: Likely Factor (TDS) to Unlikely Factor (pH, TSS)
5	Amount Major Ions, TDS, pH, TSS, and BOD Entering Navigable Water	Varies (major ions) ² 91%-92% of Initial Concentration (TDS) Similar to Background (pH) 0% of Initial Concentration (TSS) <77% of Initial Concentration (BOD)	Varies: Likely Factor (TDS) to Unlikely Factor (pH, TSS)
6	Manner or Area of Major Ions, TDS, pH, TSS, and BOD Discharge	—	—
7	Identity of Major Ions, TDS, pH, TSS, and BOD at Discharge Point	Distinct (major ions) ² 8%-9% Reduction (TDS) Similar to Background (pH) 100% Reduction (TSS) >23% Reduction (BOD)	Varies: Likely Factor (TDS) to Unlikely Factor (pH, TSS)

Notes

— = not applicable, nitrate model does not provide information about the factor

(1) Most of these parameters are above background groundwater at the Santiam River. The PHREEQC model that was used to simulate transport of these parameters does not directly evaluate transit time to the river.

(2) See Piper Diagram in Figure 7-1

(3) Geochemical results as shown reflect the base case scenario; sensitivity results are reported in Table 7-1.

Please do not hesitate to call or email if you have any questions.

Sincerely,
GSI Water Solutions, Inc.



Matt Kohlbecker, RG
Principal Hydrogeologist

Date: December 5, 2024**To:** Matt Kohlbecker, GSI Water Solutions, Inc.**CC:** Jason Keller, Geosystems Analysis, Inc.**From:** Shannon Zahuranec, Greg Lehn, James Jonas
Life Cycle Geo, LLC**Email:** shannon@lifecyclegeo.com**GEOCHEMICAL ASSESSMENT TO SUPPORT EVALUATION OF TREATED WASTEWATER INFILTRATION GATES AND MILL CITY, MARION AND LINN COUNTIES, OREGON**

1.0 Introduction

Life Cycle Geo, LLC (LCG) has prepared this report for GSI Water Solutions, Inc. (GSI) to detail the results of a geochemical assessment executed to evaluate downgradient changes in groundwater quality in support of permitting a new municipal wastewater treatment and infiltration facility in Mill City, Oregon. The proposed treatment and infiltration facility will receive wastewater from the municipal systems for Gates and Mill City, Oregon. Ultimately, the results of this assessment will be applied to inform permitting of the proposed system by the Oregon Department of Environmental Quality (DEQ). This work is subcontracted to GSI through Keller Associates by Marion County, Oregon.

2.0 Background

To support the design and permitting of the proposed wastewater treatment and infiltration facility in Mill City, Oregon, GSI previously completed a multi-phased subsurface hydrogeologic investigation (GSI 2023a, 2023b, 2023c) and a screening-level pollutant fate and transport model (GSI 2023d). The purpose and outcome of the completed assessments are summarized as follows:

- Phases I, II, and III of the hydrogeologic investigation were executed to evaluate the feasibility of constructing rapid infiltration basins (RIBs) in the Gates/Mill City area, and ultimately to select a site for the proposed RIBs. Completion of the hydrogeologic investigation entailed the construction of test pits at four candidate sites to characterize shallow soils (GSI 2023a), installation of one monitoring well at the three most favorable sites to characterize deep soils and conduct aquifer testing (GSI 2023b), and installation of two additional monitoring wells and further aquifer testing at the site selected as most favorable for the RIBs (GSI 2023c). Site GM1 was selected as the infiltration facility site based on the hydrogeologic investigation. An infiltration pilot test was conducted at GM1 during the summer of 2024 [GSI, in press].

- A screening-level pollutant fate and transport evaluation, documented in the report titled “Evaluation of the Environmental Fate of Residual Pollutants from an Advance (Class A) Treated Wastewater Infiltration System, Mill City, Oregon,” was executed using the Washington State Department of Health’s Large Onsite Septic System (LOSS) model to assess concentration changes as a function of dilution, and using the EPA’s BIOSCREEN model to assess concentration changes as a function of dispersion, biodegradation, and sorption (GSI 2023d). Concentrations of nitrate, di(2-ethylhexyl)phthalate (DEHP), and toluene were calculated in groundwater downgradient of the proposed RIBs. The downgradient concentration of all constituents was predicted to be consistent with (or below) background concentrations, except for nitrate. A concentration limit variance was determined to be appropriate based on compliance with Oregon’s groundwater quality protection requirements.

Further information on the pH, biochemical oxygen demand (BOD), total dissolved solids (TDS), and total suspended solids (TSS) of the groundwater and treated wastewater mixture at the discharge point to the Santiam River was requested by the DEQ following review of GSI’s screening-level pollutant fate and transport evaluation (GSI 2023d), which is the focus of the current geochemical modeling assessment (DEQ 2024a).

The character of the groundwater that ultimately discharges to navigable waters informs the functional equivalence test as required by the April 2020 U.S. Supreme Court Decision in *County of Maui, Hawaii v. Hawaii Wildlife Fund, et al.* The discharge must not “maintain enough similarity to the original effluent from the facility” to be permitted under a Water Pollution Control Facility permit (WPCF) in the State of Oregon (DEQ 2024b). The Oregon Department of Environmental Quality provides guidance on determining if discharges for a specific project are functionally equivalent, following the April 2020 decision (DEQ 2024b).

3.0 Objective

The purpose of this geochemical assessment was to evaluate, specifically, the transport and evolution of the proposed RIB effluent with respect to pH, TDS, BOD, and TSS as it mixes with groundwater and flows downgradient. This assessment was completed to inform the functional equivalence test for the proposed treated wastewater infiltration. As part of this evaluation, a one-dimensional reactive transport geochemical model was prepared to simulate the mixing of wastewater effluent from the RIBs with background groundwater and the interactions of the water mixture with site precipitation, soil gases, and aquifer solids along the travel path to the Santiam River.

4.0 Site Description

Site GM1, selected for the proposed infiltration facility, is located on the eastern edge of Mill City, Oregon, (Figure 4-1). The total size of the RIBs will be approximately 2.04 acres (six individual basins at approximately 0.34 acres per basin) and will be constructed on a relatively flat bench on the north side of the GM1 site at an elevation of 850 ft above mean sea level (amsl). The distance between the RIBs and the Santiam River along the groundwater flowpath is about 1,900 feet (the distance between the river and the nearest corner of the facility). The shallow soils of the GM1 site consist of approximately one to two feet of sandy loam soil underlain by a heterogeneous mix of sandy loam, loamy sand and sandy soils with coarse gravel, cobbles, and boulders, consistent with fluvial deposition. Seasonal high groundwater is present at approximately 10 to 15 feet below ground surface (ft bgs) at GM1 (GSI, 2024a) and flows northwest towards the Santiam River at a rate of approximately 2.85 ft per day.

5.0 Geochemical Characterization

To support the geochemical evaluation of pH, TDS, BOD, and TSS, aqueous-phase and solid-phase geochemical data were collected by GSI in spring 2024. The available data and results are described in the following subsections.

5.1 Aquifer Solids

5.1.1 Methodology

Twelve solid samples were collected from the well boring of GM1-MW4 to support this geochemical assessment (Figure 5-1). The samples were collected and composited from each five-foot interval along the length of the well boring. Prior to analysis, aquifer solid samples were sieved to exclude material greater than 2 mm in diameter, prioritizing the characterization of the finer fractions that comprise the majority of the reactive mineral surfaces. Based on drill logs, approximately 80% of the aquifer solids were logged as gravel (greater than 2 mm in diameter) and the remaining 20% was logged as sand, silt, or clay (Attachment 1).

Bulk solid characterization for the twelve aquifer solids samples was completed at ACZ Laboratories (Steamboat Springs, CO), detailed in Tables 5-1 through 5-3, included the following testing:

- **Acid base accounting (ABA):** ABA static testing aims to predict the acid-generating, and the pH neutralizing potential of materials, which informs assessment of the geochemical interaction between the aquifer solids, the upgradient groundwater, and the RIB water. This involves determining the acid generation potential (AGP), which is calculated using the sulfur content (total sulfur and/or pyritic sulfur), and the acid neutralization potential (ANP) assessed through titration with a strong acid.

- **Total metals:** a measure of bulk concentration determined by the acid digestion of the soil, and indication of which metals are present and enriched within the solid phase materials.
- **Cation exchange capacity (CEC):** The CEC describes the capacity of a soil to exchange positively charged ions with ions in groundwater, aiding in understanding aquifer capacity for undergoing ion exchange reactions. The CEC is dependent on organic matter, types and quantity of clay materials, and metal oxides.
- **Mineralogy by X-ray diffraction (XRD):** Mineralogy by XRD quantifies crystalline minerals phases with Rietveld refinement, which offers increased precision in quantification calculations. Identifying mineral phases aids in understanding mineral precipitation and dissolution reactions, attenuation mechanisms, and aquifer attenuation capacity.

A subset of four samples were selected for more advanced geochemical testing:

- **Sequential extraction procedure (SEP):** The SEP testing was conducted according to the methods of Tessier et al., (1978). This testing quantifies the amounts of key metals associated with different operationally-defined fractions of the solid. Initial extractions target loosely bound, exchangeable metals, representing the proportion that is more likely to become mobile under near-surface environmental conditions. Subsequent sequential leaching steps progressively extract metals associated with increasingly more recalcitrant fractions of the soil, including carbonate minerals, amorphous and crystalline metal oxy-hydroxides, organics, and silicates. This method allows for a nuanced understanding of metal partitioning with various phases in the soils, aiding interpretation of conditions that may contribute to metal attenuation or release. Iron, manganese, and aluminum were analyzed in the leachates due to their relevance for interpreting geochemical conditions and because they form the basis of the dominant adsorbent minerals in the aquifer matrix (iron, manganese, and aluminum oxy-hydroxide).

5.1.2 Results

Laboratory reports from ACZ Laboratories (ACZ) are presented in **Attachment 2**. Tabulated geochemical results are provided in **Table 5-1**, **Table 5-2**, and **Table 5-3**.

- **Acid Base Accounting (ABA)** - ABA results, shown in **Table 5-1**, indicate total sulfur and sulfide sulfur were below detection in all samples, suggesting both negligible sulfide oxidation and negligible acid generation potential from aquifer solids. The ANP for the collected samples was relatively low, ranging from 9 to 11 tons calcium carbonate equivalent per kiloton (t CaCO₃/kt) in aquifer solids above the water table and from 14 to 26 t CaCO₃/kt for aquifer solids below the water table. The lack of AGP and moderately low ANP indicates the aquifer solids have a low potential to generate acid and limited capacity to buffer against potential changes in pH. The measured paste pH values were relatively low in the samples above the water table (pH = 5.8 to 6.6 standard units, or SU), likely reflecting the slightly acidic precipitation in equilibrium

with atmospheric carbon dioxide (pH = 5.2 to 5.5 SU) without the presence of acid neutralizing minerals, elevated concentrations of soil carbon dioxide in the subsurface, or a combination of both.

- **Total Metals** - The trends in total metals concentrations in the aquifer solids were evaluated to understand the different geochemical environments (**Table 5-1**). Calcium, phosphorus, and sodium are depleted above the water table, relative to samples below the water table. Aluminum, arsenic, barium, iron, and manganese were enriched above the water table relative to samples below the water table. This pattern indicates the accumulated effect of mineral weathering on the shallow unsaturated soils, potentially exposed to higher concentrations of soil carbon dioxide, compared to the saturated zone. The flushed cations and enrichment of metals typically present in oxy-hydroxide minerals indicates higher weathering rates in the unsaturated zone.
- **Mineralogy** - Soil samples were primary composed of largely unreactive silicate minerals (plagioclase, quartz, pyroxene) and secondary aluminosilicate clay (smectite, chlorite) minerals (**Table 5-2 and Figure 5-2**). Clays were generally more abundant at the surface and the abundance decreased with depth. Deeper samples had a higher proportion of primary silicates (plagioclase and quartz). Trace amounts of iron oxy-hydroxide minerals (hematite) were detected at trace levels (approximately 1%) in four out of the seven samples.
- **Cation Exchange Capacity** - Higher CEC values were detected in the shallower soils (GM1-MW4 6-8, GM1-MW4 9-10, GM1-MW4 10-11), with values ranging between 17.7 to 22.3 meq/100g (**Table 5-2**). In the deeper portions of the aquifer, samples ranged from 5.6 to 7.9 meq/100g. Samples with the greatest composition of smectite also had the highest CEC, but the relationship is non-linear.
- **Sequential Extraction Procedure** - The SEP analytical results for iron, aluminum, and manganese are provided in **Table 5-3** and graphically in **Figure 5-3**. As a quality assurance and quality control (QA/QC) check, the sum of metals extracted in each SEP step were compared against the total digestion of the soil by USEPA method 3050. The sum of the SEP steps were within +/-11% of the total soil concentration for each sample and analyte, indicating strong quality control between the two results obtained from different analytical methods. Most iron, aluminum, and manganese was associated with the Step 5 and Step 6 fractions, which are generally considered the least reactive fractions. The concentrations of iron, aluminum, and manganese in SEP Steps 3 and 4 are interpreted to be associated with metal oxy-hydroxide minerals, which represent the sorption capacity within the aquifer solids. Between 7.8 and 13.6% of iron, 0.3 and 1.5% of aluminum, and 14.4 and 40.3% of manganese was present in soils

as metal oxy-hydroxide minerals. Consistent with the total metals results, greater quantities of iron, aluminum, and manganese-bearing adsorptive mineralization was present in the unsaturated zone relative to the saturated zone samples analyzed.

5.2 Water Quality

5.2.1 Methodology

The aqueous-phase data collected for the geochemical assessment include groundwater and current treatment plant influent water. Sampling locations are presented in **Figure 5-1**. Sampling methods are described in *Gates/Mill City Water Quality Sampling and Analysis Technical Memorandum* (GSI, 2024a). The available data is provided in **Table 5-4** and summarized as follows:

- **Groundwater** - The groundwater quality sample results available for incorporation to the geochemical assessment include four samples collected in 2023 from groundwater monitoring wells GM1-MW1, GM1-MW4¹, and GM1-MW5¹, and three samples collected in 2024 from GM1-MW1, GM1-MW2, and GM1-MW4. The sample collected from GM1-MW4 in 2024 represented the most complete analytical suite of field parameters, major ions, and metals. The GM1-MW1 sample from 2023 and GM1-MW2 sample from 2024 had less complete analyte suites but were sufficient to evaluate the variability in groundwater quality in this geochemical evaluation. The monitoring well locations are shown in **Figure 5-1**.
- **Treatment Plant Influent Water** - A simulated infiltrated water quality was produced from available influent water quality data from the existing wastewater treatment plant in combination with the effluent design criteria established for the proposed treatment plant (Keller 2024a). Available data included two influent water quality samples collected May 2023 and May 2024 (**Table 5-4**).

5.2.2 Results

Groundwater and treatment plant influent water quality results are discussed, as follows:

- **Groundwater** - The groundwater quality measured from GM1-MW1, GM1-MW2, and GM1-MW4 reflected a circumneutral field pH ranging from 6.3 to 6.5 SU with bicarbonate alkalinity ranging from 42 to 77 milligrams per liter (mg/L) as calcium carbonate (CaCO₃). TDS concentration was low in the groundwater samples, ranging from 78 to 115 mg/L, and composed predominantly of bicarbonate and calcium with lower relative proportions of other major ions (magnesium, sodium, potassium, chloride, sulfate). TSS was measured at 11.5 mg/L in the groundwater sample from GM1-MW4. This TSS value is unlikely to be representative of

¹ Results from samples GM1-MW4 and GM1-MW5 collected in 2023 did not have a full suite of major cations and anions and are not included in Table 5-4, but results for these samples can be found in GSI, 2024a.

the aquifer TSS based on the high turbidity of this sample, which is a field parameter closely related to TSS, of 25 nephelometric turbidity units (NTU) compared to the low turbidity measured in other groundwater samples (2 to 5 NTU). Overall, dissolved metals concentrations are low in the groundwater samples.

The redox condition of the groundwater samples is interpreted as oxidizing, with oxidation reduction potential (ORP) measurements ranging from 94 to 189 millivolts (mV), generally low concentrations of dissolved iron and manganese, and ammonia nitrogen was below detectable limits (0.02 mg N/L). Concentrations of nitrate nitrogen were overall low, ranging from 0.3 to 1.1 mg/L.

- **Treatment Plant Influent** - The overall disposition of water quality reporting to the water treatment plant is similar to groundwater in terms of a neutral pH and generally low concentrations of dissolved metals. Despite broad similarities, several key differences in water quality are observed for the water reporting to the existing wastewater treatment plant relative to the observed groundwater. Namely, ammonia reflects a higher concentration in the range of 50 mg N/L, TDS is approximately three times higher in influent water relative to groundwater (307 mg/L compared with 78 to 115 mg/L, respectively), phosphorous is elevated at 6 mg/L, and alkalinity is reported to be higher in the range of 296 to 340 mg/L as CaCO₃. In addition, review of the 2022 Discharge Monitoring Reports (DMRs) for the existing treatment plant indicates that BOD and TSS are elevated in the influent water with an annual average of 132 mg/L and 33 mg/L, respectively.

Discussion of the treatment processes and adjustments that will reflect in effluent water quality are discussed in Section 6.1.

6.0 Geochemical Modeling

To predict the geochemical evolution of the RIB effluent as it enters the vadose zone, mixes with the regional groundwater, interacts with aquifer solids, and travels downgradient, a one-dimensional reactive transport geochemical model was developed. The primary focus of this model is to simulate the processes that affect water chemistry along the flow path from the RIBs downgradient to the Santiam River, with emphasis on key parameters pH, TDS, and BOD. This approach ensures a comprehensive understanding of water quality evolution in the subsurface system.

6.1 Conceptual Site Model

This geochemical conceptual site model (CSM) identifies key hydrogeological and geochemical processes necessary for simulating the fate and transport of constituents in the RIB effluent. The CSM is divided into three main components:

- **Wastewater Treatment System:** The proposed wastewater treatment system introduces key chemical modifications to the treated wastewater before it is discharged to the RIBs. The primary modifications include aeration to oxidize ammonia, sodium hydroxide (NaOH) for pH control, and methanol addition for the removal of nitrate. These processes result in changes in water quality for many constituents, including the following changes to key parameters (Keller 2024b):
 - pH: adjusted to approximately 7.00 SU with NaOH
 - Nitrate: reduced to 1 mg/L
 - Ammonia: reduced to 1 mg/L
 - TSS: reduced to 20 mg/L
 - BOD: reduced to 20 mg/L
 - Alkalinity: reduced to 80 mg/L as CaCO₃
 - Sodium: increased by up to 5 mg/L
- **Infiltration at the RIBs:** The treated effluent is discharged to the RIBs, where it mixes with precipitation falling over the facility and equilibrates with atmospheric gases before infiltrating into the vadose zone. Oversaturated minerals, including calcite, gypsum, ferrihydrite, gibbsite, and manganite are allowed to precipitate within the RIBs, and pH and redox conditions are equilibrated accordingly. These minerals were selected due to pH buffering capacity (calcite), for presence as common scaling minerals (gypsum and ferrihydrite) and all for being minerals with relatively fast reaction kinetics that are relevant in the circumneutral waters expected within the RIB and underlying groundwater. Ferrihydrite, gibbsite, and manganite represent relatively amorphous phases with high surface area that are known sorbents. The infiltration is assumed to occur at a constant flow at the center of the facility.
- **Interaction along the Flow Path:** After infiltrating, the effluent moves through the vadose zone, mixes with upgradient groundwater, and flows downgradient to the Santiam River. Along this flow path, the mixture equilibrates with soil gases, and interacts with aquifer solids, including processes such as adsorption, cation exchange, and mineral dissolution/precipitation. Infiltrating precipitation also will mix into groundwater along the flow path, providing an additional source of dilution.

6.2 Modeling Approach

The geochemical processes identified in the CSM were simulated using PHREEQC, an industry standard software developed by the United States Geological Survey (USGS) for modeling geochemical reactions and processes. PHREEQC allows for the simulation of geochemical reactions such as thermodynamic equilibrium, mineral dissolution/precipitation, ion exchange, sorption, and one-dimensional transport along the flow path (Parkhurst and Appelo, 2013). The United States Environmental Protection Agency

(USEPA) Minteq.v4 thermodynamic database was used for this model (USEPA 1998), updated with adsorption coefficients for iron, aluminum, and manganese oxy-hydroxide minerals compiled from the PHREEQ-N-AMDTreat database (Cravotta 2020). Longitudinal dispersivity and flow velocity are additionally accounted for in the one-dimensional, geochemical reactive transport model simulation; however, vertical and transverse dispersivity are not.

The model is structured into five stages to represent the key steps in the flow path:

1. **Mixing with precipitation:** Treated effluent water in the RIB is blended with the average site precipitation (rain and snow) falling within the facility.
2. **Equilibration within the RIB:** The effluent is equilibrated with atmospheric gases, resulting in the precipitation of supersaturated minerals and the adsorption of dissolved ions.
3. **Equilibration within the Unsaturated Zone:** As the water moves through the unsaturated zone, it interacts with soil gases and minerals, potentially leading to additional mineral precipitation/dissolution, adsorption/desorption and ion exchange. The solids composition in the unsaturated zones is represented by soil samples GM1-MW4 6-8, GM1-MW4 9-10, and GM1-MW4 10-11 (Section 5.1).
4. **Mixing with Groundwater:** Upon reaching the saturated zone, the effluent mixes with regional groundwater. Mixing is assumed to be complete in the saturated zone beneath the RIBs.
5. **Equilibration within the Saturated Zone:** The water interacts with the saturated zone aquifer solids, leading to further geochemical transformations such as ion exchange and mineral dissolution. The solids composition in the saturated zones is represented by soil samples GM1-MW4 13-15, GM1-MW4 16-20, GM1-MW4 20-23, and GM1-MW4 25-26 (Section 5.1).
6. **Transport along the Flow Path:** As the water flows downgradient, it continues to undergo geochemical changes. Dilution along the flow path is anticipated due to additional infiltrating precipitation. Along the transect, the effluent groundwater mixture interaction with the saturated zone solids are key processes modeled in this step.

6.3 Key Geochemical Parameters Evaluated

The focus of this evaluation is on the following key parameters:

- **pH** influences (and is influenced by) many geochemical processes, including mineral solubility, speciation, and microbial activity. The geochemical model simulates pH by accounting for acid-base reactions, redox reactions, carbonate equilibria, and the influence of dissolved gases like carbon dioxide. Monitoring pH along the flow path provides insight into potential chemical reactions such as mineral dissolution and precipitation.
- **Total Dissolved Solids (TDS)** is modeled by summing the concentrations of individual ions such as calcium, magnesium, sodium, chloride, sulfate, and bicarbonate. The geochemical model

predicts changes in TDS resulting from mineral dissolution/precipitation, ion exchange, and adsorption along the flow path to the Santiam River.

- **Biochemical Oxygen Demand (BOD)** was evaluated semi-quantitatively through the comparison of available oxygen consuming compounds (ammonia and organic carbon) to the amount of available dissolved oxygen present in the groundwater. The model tracks the transition from the reduced species of ammonia to the oxidized nitrate species, which is indicative of oxidation with atmospheric oxygen, soil oxygen, and dissolved oxygen in groundwater along the flow path.
- **Total Suspended Solids (TSS)** was not handled directly within the geochemical model, as transport of TSS within the subsurface is primarily a function of physical processes. However, given that TSS is likely to be composed predominantly of suspended organic matter, it is considered within the context of the BOD assessment.

6.4 Input Parameters

The following sections describe the input parameters used in the reactive transport and an explanation of their sources and justification.

6.4.1 Initial Solutions

The initial water qualities input into the model for site precipitation, background groundwater, and treated effluent are provided in **Table 6-1**.

Precipitation quality in the model is estimated using the annual average major ion quality measured at the National Atmospheric Deposition Program (NADP) H.J. Andrews Experimental Forest monitoring site (NTN Site: OR10) between 1980 and 2023, which is located approximately 40 miles southeast of Mill City, Oregon.

The upgradient groundwater solution was primarily based on the water quality sample collected from GM1-MW4 on April 25, 2024, with several adjustments. TSS and iron were not analyzed on the sample collected from GM1-MW4 on April 25, 2024. To include these parameters, the TSS and iron concentrations were substituted from the sample collected at GM1-MW1 on May 28, 2023. In addition, the background nitrate concentration was set to 0.56 mg N/L, to match the long-term average nitrate concentration observed in background groundwater [GSI, 2024c].

The wastewater treatment effluent concentrations were based on a representative influent sample collected from the current wastewater treatment plant on May 1st, 2024, with several adjustments to reflect the changed condition of the wastewater following treatment by the proposed system. This sample was selected because it had the most complete analyte list for geochemical modeling (pH, conductivity, major ions, metals/metalloids). As discussed in Section 6.1, the effluent pH, nitrate, ammonia, and TSS were set to the required treatment levels. As part of the treatment process, the

alkalinity of the solution is expected to decrease to 80 mg CaCO₃/L and the concentration of sodium may increase up to 5 mg/L due to the adjustment of pH using NaOH; (Communication with Keller Associates, Inc. on July 2, 2024). The removal of nitrate, ammonia, and alkalinity will result in a decrease in TDS, which is calculated to be approximately 223 mg/L following treatment for the base case.

As lead concentrations were not measured on the sample from May 2024, the lead concentration from the influent sample collected on May 2, 2023 was used (<0.0002 mg Pb/L). For all solutions, when a constituent in a measured source was measured at a concentration below the detection limits, the value was replaced with a concentration equal to one half the detection limit.

Solutions were charge balanced on bromide for modeling to avoid computational artifacts. Bromide was below detection in both background groundwater and influent. Bromide was selected over chloride because it is a trace anion and not included when evaluating the major ion signature of a sample. The intent was to avoid picking a constituent that could create a modeling artifact that could affect conclusions about the groundwater signature reaching the Santiam River.

6.4.2 Mixing and Dilution

At two places in the reactive transport geochemical model, the RIB effluent is mixed with another water source and diluted:

- The first dilution occurs as effluent mixes with precipitation that falls into the RIBs. Using details provided in GSI 2024b, the model simulates approximately 237,000 gallons per day of water (conservatively the 2045 projected annual average wet weather flow rate) from the treatment plant mixing with approximately 5,257 gallons per day of net precipitation (precipitation minus evaporation) falling over the RIBs. This results in a mixture that is 97.8% RIB effluent and 2.2% precipitation.
- The second mixing/dilution step occurs as the infiltrating water mixes with groundwater underneath the RIBs. Using details provided in GSI 2024b, the model simulates approximately 242,257 gallons per day (effluent + basin net precipitation) mixing with approximately 28,994 gallons per day of upgradient groundwater. This results in a mixture that is 89.1% RIB effluent plus basin net precipitation and 10.7% background groundwater.
- The final dilution occurs as the effluent-groundwater moves downgradient toward the Santiam River. The net precipitation (precipitation minus evaporation) that falls over the flow path is expected to be approximately 57,822 gallons per day. Since the precipitation will interact with unsaturated soils, the composition is approximated using the background groundwater. This final dilution results in a mixture that is 82.4% RIB effluent-groundwater mixture and 17.6% background groundwater/precipitation.

Combining all the mixing/dilutions steps, the final solution reaching the Santiam River is 72.0% RIB Effluent, 1.7% direct precipitation into the RIBs, 8.8% upgradient groundwater, and 17.6% infiltrating precipitation along the flow path, prior to modifications due to mineral precipitation/dissolution and interactions with aquifer solids (sorption and cation exchange).

6.4.3 Gases

Within the RIBs, atmospheric gases carbon dioxide and oxygen were set to 410 ppm and 21%, respectively.

Within the unsaturated and saturated zone, soil carbon dioxide and oxygen levels are assumed to be 4,000 ppm and 5%, respectively, reflecting a mixture of atmospheric gas concentrations and the gas saturation levels observed in upgradient groundwater samples (CO_2 = approximately 15,000 ppm and O_2 = approximately 3%).

The elevated partial pressures of carbon dioxide in equilibrium with background groundwater samples (GM1-MW1, GM1-MW2, and GM1-MW4) indicate that the saturated zone is a closed system, with minimal exchange with overlying unsaturated soils. For that reason, the saturated flow path was modeled without gas exchange.

6.4.4 Mineral Precipitation/Dissolution

At each stage of the model described in Section 6.2, the water interacts with aquifer solids and precipitates oversaturated minerals and dissolves undersaturated minerals. As discussed in Section 6.1, the majority of the less than 2 mm fraction soils are primary silicates and clays, have generally slow dissolution rates at the circumneutral pH values, and would be expected to make minor contributions to groundwater. Only hematite was identified by XRD as an iron oxide mineral that could potentially be expected to dissolve over shorter timescales. The SEP results generally confirm the presence of low levels of amorphous and crystalline iron oxy-hydroxides (including, but not limited to hematite), as well as low levels of aluminum and manganese oxy-hydroxides. The concentrations identified would generally be lower than the detection limits of XRD.

LCG reviewed the saturation of minerals in upgradient groundwater and the predicted effluent to determine what common minerals should be included for precipitation and dissolution in the model. Given the low concentrations of most constituents in both waters, the waters are unlikely to be controlled by large scale precipitation of most minerals. The following list of common minerals was identified as a likely list of reacting minerals for this circumneutral environmental setting:

- Calcite
- Gypsum
- Ferrihydrite
- Gibbsite
- Manganite

Calcite and gypsum were not identified in aquifer solids by mineralogy and background groundwater qualities were undersaturated with respect to these minerals. As discussed above, the SEP results suggest the presence of minor amounts of amorphous and crystalline iron, aluminum, and manganese oxy-hydroxides. Assuming all the iron, aluminum, and manganese were present as ferrihydrite, gibbsite, and manganite, respectively, initial concentrations of these minerals were estimated for the unsaturated and saturated portion of the soils (**Table 6-2**).

6.4.5 Adsorption to Metal Oxy-Hydroxide Minerals

Dissolved constituents in groundwater also interact with adsorption sites on metal oxy-hydroxide minerals, altering the composition of groundwater. The adsorptive partitioning between dissolved and solid phases was simulated using a two-layer surface complexation model included in PHREEQC. Sorption was parameterized for iron (hydrous ferric oxide [Hfo]; Dzombak and Morel [1990]) as ferrihydrite [$\text{Fe}(\text{OH})_3(\text{am})$], aluminum (hydrous aluminum oxide [Hao]; Karamalidis and Dzombak [2011]) as gibbsite [$\text{Al}(\text{OH})_3(\text{am})$], and manganese (hydrous manganese oxide [Hmo]; Tonkin et al. [2004]) as manganite [$\text{Mn}(\text{OH})_3(\text{am})$].

The Hfo, Hao, and Hmo surface properties (i.e., surface area, site density, and types of sites) from Dzombak and Morel (1990), Karamalidis and Dzombak (2011), and Tonkin et al. (2004) are provided in **Table 6-3** and were used to parameterize the amount of iron, aluminum, and manganese adsorption sites per mole of each mineral.

The amount of Hfo, Hao, and Hmo available for attenuation was determined dynamically in the model, with the initial concentrations of Hfo, Hao, and Hmo based on the initial amounts of ferrihydrite, gibbsite, and manganite observed in aquifer solids, and the precipitation or dissolution of these minerals in effluent and effluent-groundwater mixtures increasing or decreasing the quantity accordingly. As discussed above, only 20% of the soil mass was comprised of sand, silt, and clay (<2 mm diameter), which makes up the majority of the reactive surfaces in the soil and was the focus of the geochemical characterization program. For this reason, only 20% of the soil beneath the RIBs and along the flow path to the Santiam River was modeled to have the capacity for sorption.

At the start of the model simulation, the sorption sites were set to be in equilibrium with background groundwater concentrations (**Table 6-1**). As the groundwater quality shifts to reflect the mixture of effluent and groundwater, the constituents bound to the sorption sites re-equilibrate.

6.4.6 Cation Exchange Capacity

In addition to adsorption to metal oxy-hydroxides minerals, clay minerals also have cation exchange sites that can equilibrate with groundwater and alter the concentrations of certain constituents in groundwater. The site mineralogy results indicate that between 36 and 53% of the less than 2mm fraction of soils were composed of smectite clay. This is consistent with the CEC detected during

aquifer solids characterization (5.6 to 22.3 meq/100g)². As discussed for adsorption (Section 6.4.5), only 20% of the soil beneath the RIBs and along the flow path to the Santiam River was modeled to have capacity for cation exchange.

At the start of the model simulation, the CEC sites were set to equilibrium with background groundwater concentrations (Table 6-1). As the groundwater quality shifts to reflect the mixture of effluent and groundwater, the constituents bound to the CEC sites re-equilibrate.

6.4.7 Reactive Transport

After the second dilution from precipitation along the flow path, the water was transported through the one-dimensional reactive transport simulation. The water is simulated to travel from the saturated zone beneath the RIBs nearest to the Santiam River to the river (1,898 ft total) divided for the model into 190 separate 10 ft cells. As a one-dimensional model, the simulation assumes no lateral dispersion and the aquifer is vertically well mixed over the travel path to Santiam River. The flow parameters were selected and calibrated in the development of the MODFLOW model in GSI 2024b. The flow velocity was set to 3.33 ft/day, corresponding to approximately 3.00 days for movement of water from one cell to the next. The simulation was run for 20 years.

Each 10 ft cell is simulated to have the initial mineral masses of ferrihydrite, gibbsite, and manganite, the corresponding sorption sites associated with these metal oxy-hydroxide minerals (Hfo, Hao, and Hmo), and CEC sites for the saturated aquifer solids (Section 5.1). The sorption and CEC sites were equilibrated with background groundwater for the initial conditions at the start of the simulation.

6.4.8 Sensitivity Analyses

In addition to the Base Case described above, four additional sensitivity analyses were performed to understand dependency of the model on the variables of pH, infiltration ratio, and nitrate concentration. For each sensitivity evaluated, the base case was held constant with one variable adjusted according to the following:

- **Sensitivity #1-** The pH of RIB effluent was reduced to the minimum allowable level (pH 6.5 SU). The pH of the Base Case effluent was adjusted with the removal of sodium hydroxide, simulating less being added during the treatment process.
- **Sensitivity #2-** The pH of RIB effluent was increased to the maximum allowable level (pH 8.5 SU). The pH of the Base Case effluent was adjusted with the model using sodium hydroxide,

² The CEC concentrations were converted for use in PHREEQC according to the following equation:

$$\left(\frac{\text{meq CEC}}{100 \text{ g of sand/fines}}\right) * \left(\frac{0.2 \text{ kg of fines}}{1.0 \text{ kg of bulk soil}}\right) * \left(\frac{\text{eq CEC}}{1000 \text{ meq CEC}}\right) * \left(\frac{200 \text{ g of sand/fines}}{1 \text{ kg of soil}}\right) * \left(\frac{\text{kg of soil}}{\text{L of soil}}\right) * \left(\frac{1}{\text{porosity}}\right) = \left(\frac{\text{eq CEC}}{\text{L of water}}\right)$$

which is expected to be used in the plant to adjust the pH during secondary treatment, prior to tertiary denitrification and disinfection.

- **Sensitivity #3-** The infiltration rate of effluent in the RIBs was increased from the Base Case of 237,000 gallons per day (based on the 2045 annual wet weather flow rate) to 262,000 gallons (based on the 2045 maximum month wet weather flow rate).
- **Sensitivity #4-** The nitrate concentration in effluent is modeled to be 5 times higher (5 mg N/L) than the Base Case.

6.5 Assumptions and Limitations

The following assumptions are associated with the geochemical model:

- The infiltration is assumed to occur at a constant flow at the RIB located downgradient of the facility.
- Within each cell of the model, geochemical reactions reach thermodynamic equilibrium. No reaction kinetics were included that may reduce the mineral dissolution or precipitation rates.
- Aquifer solids are assumed to be homogeneous and consistent with the samples collected from GM1-MW4 borehole.
- Upgradient groundwater is assumed to be constant and consistent with the sample collected from GM1-MW4 (with the modifications described above).
- Effluent water quality is simulated based on available data and understanding from the proposed treatment system.
- For measured water quality data within the modeling scenarios, samples measured below the detection limit were simulated at one half the detection limit.

7.0 Results and Discussion

Water quality predictions are provided in **Table 7-1**, showing the water quality at Santiam River at 5 years, 10 years, and 20 years for the base case and four sensitivity analyses.

The major ion signatures of the background groundwater, RIB effluent, and groundwater at the Santiam River for the base case and sensitivities are shown on a Piper Diagram in **Figure 7-1**. As RIB-influenced groundwater reaches the Santiam River, the groundwater quality starts to shift in response to introduction of effluent water from the RIBs to the regional groundwater. Due to the combined influences of mineral precipitation, adsorption, and cation exchange, mixtures of the background groundwater, RIB effluent, and precipitation do not fall on a linear mixing line, and instead follow a curved mixing line. Over the 20 years of the modeled simulation, the major cations are predicted to trend towards a similar proportion to background groundwater (calcium and magnesium dominated). The proportions of anions are more similar to effluent (still bicarbonate-dominated, but with higher concentrations of chloride and sulfate). As the aquifer solids were initially equilibrated with background

groundwater, the cations on the sorption and exchange sites had a large proportion of calcium relative to sodium. Once the sodium-dominant effluent-influenced groundwater starts interacting with the sorption and cation exchange sites, a proportionally larger amount of sodium is sorbed to the solids, which releases calcium into the groundwater. The calcium on the sorption and cation exchange sites is partially depleted over the 20 years, but a residual effect remains.

In addition to the evolution of the major ion signatures of the effluent-influenced groundwater at Santiam River, the trace metal signature is also altered over the flow path. **Figure 7-2** presents a Radar Diagram, showing the relative concentrations of key trace metals (arsenic, barium, chromium, copper, nickel, and zinc) in background groundwater, effluent, and effluent-influenced groundwater at the Santiam River after 5 years, 10 years, and 20 years. These specific constituents were selected because they have relatively low concentrations in the background groundwater and higher concentrations in the effluent. The predicted concentrations of these constituents at the Santiam River were lower than the effluent due to the uptake of these constituents by adsorbent minerals in the soils along the flow path. This figure shows that dilution and sorption can have a large effect on the concentration of other constituents in the effluent-influenced water and change the nature of the effluent over the travel path to the Santiam River.

The pH predicted for groundwater arriving at the Santiam River is neutral, and ranges between 6.8 and 6.9 S.U. over the 20-year modeling period, generally at an intermediate value between the two primary water sources (effluent and background groundwater). Similarly, the TDS of groundwater at the Santiam River is predicted to vary between 203 to 206 mg/L over the 20-year modeling period, an 8 to 10 % decrease compared to the effluent concentration. The lower TDS values are driven by dilution and the altered proportions of cations contributing to TDS. The biggest differences are observed in the early years of the modeling period, and higher pH and TDS values are expected after 10 years of operations, as adsorption sites reach a new equilibrium with the effluent-influenced water.

Ammonia concentrations were predicted to be extremely low in the oxidizing groundwater and primarily converted to nitrate concentration, which were consistently predicted at approximately 1.7 mg N/L throughout the 20-year modeling period. This reaction is most likely mediated by autotrophic bacteria that convert ammonia to nitrite then nitrite to nitrate under aerobic conditions (the biological processes are assumed to occur based on fundamental understanding but are not directly modeled). Denitrification (the conversion of nitrate to nitrogen gas) was not modeled within the groundwater but would contribute to further decreases in both nitrate and BOD as a result.

Transport of TSS was not handled directly within the geochemical model simulations. The transport of TSS in groundwater is governed by the physical and chemical characteristics of both the geologic material and the water itself. As groundwater flows through unconsolidated materials such as sand, silt, and clay, TSS is typically removed due to a combination of filtration, sedimentation, and adsorption. Additionally, TSS is assumed to be primarily suspended organic matter from the proposed

treatment plant, in this case, and would thus be additionally subjected to the process of oxidation. Filtration occurs when larger particles are physically trapped in pore spaces, while finer particles settle out of suspension under gravity in regions where flow velocities decrease. Additionally, electrostatic forces cause colloidal particles to adhere to mineral surfaces through the chemical mechanisms of adsorption and exchange, further reducing TSS concentrations along the flow path. These mechanisms are well-documented in studies of porous media transport, where researchers such as Bradford et al. (2006) have observed the retention of particles in saturated environments, confirming that the gradual attenuation of TSS is a natural function of subsurface flow through heterogeneous geologic material.

BOD generally reflects the concentration of reduced forms of nitrogen (ammonia and/or nitrite) and organic carbon available for abiotic and microbial oxidation, which can consume oxygen. As the treatment system is designed for effluent to have 20 mg/L BOD, mechanisms that decrease the concentrations of reduced nitrogen form or organics along the flow path have the potential to reduce the BOD concentrations. Given the well oxygenated RIB effluent and partially oxygenated unsaturated and saturated zones, the model predicts all ammonia and nitrite are converted to nitrate along the flow path. The conversion of ammonia (1 mg N/L) to nitrate, alone, will result in a reduced BOD of 4.6 mg/L³ or approximately a 23% reduction of the expected effluent discharge concentration (20 mg/L). With the RIBs and soils expected to remove a large proportion of organic carbon in the form TSS, the BOD will decrease even further. The combined removal of ammonia by oxidation and TSS by physical filtration is expected to fully consume BOD prior to reaching the Santiam River.

Results of the sensitivity analyses are also shown in **Table 7-1**, **Figure 7-1**, and **Figure 7-2**. Generally, the model was relatively insensitive to effluent pH (within the range of allowable discharges), small changes in RIB infiltration rate, and the model-assessed nitrate concentrations. On the Piper Diagram and Radar Diagram, the concentrations and signatures under sensitivity analyses are nearly identical to the Base Case. The effluent pH has a small effect on which metals will precipitate and adsorb, and therefore, a small effect on the pH and TDS concentrations at Santiam River, but minimal difference compared to the scale of geochemical evolution of the effluent in the Base Case. The equilibration of RIB water with atmospheric and soil carbon dioxide, as well as the carbonate alkalinity in the background groundwater quickly moderates the lower and higher pH predicted in Scenarios #1 and #2 (effluent pH of 6.5 and 8.5 S.U., respectively). The RIB effluent flow in Scenario #3 was only approximately 10 % higher than the Base Case and is only a 2 % larger share of the water that reaches the Santiam River. For this reason, Scenario #3 is nearly indistinguishable from the Base Case. Scenario

³ The change in BOD from the conversion of ammonia to nitrate was completed by the following equation:

$$\left(\frac{1 \text{ mg } NH_3 \text{ as } N}{L}\right) * \left(\frac{1 \text{ mmole } NH_3}{14.01 \text{ mg } NH_3 \text{ as } N}\right) * \left(\frac{2 \text{ mmoles } O_2}{1 \text{ mmole } NH_3}\right) * \left(\frac{32.00 \text{ mg } O_2}{1 \text{ mmole } O_2}\right) = \frac{4.6 \text{ mg } O_2 \text{ consumed}}{L \text{ of water}}$$

#4 has a higher nitrate concentration discharging into the Santiam River (4.6 mg N/L), but this has a negligible effect on the major ion signatures, TDS, pH, or BOD predictions. While higher nitrate concentrations are considered in the sensitivity analysis, the assessed concentration of nitrate is understood to be five times greater than the expected effluent concentration for the proposed treatment facility.

8.0 Conclusions

LCG makes the following conclusions based on the geochemical model simulations assessed:

- The major ion and trace metal signatures of effluent-influenced water shift over the flow path from the RIBs to the Santiam River, primarily driven by cation exchange, sorption, mineral dissolution/precipitation, and dilution. The altered signatures in groundwater no longer directly resemble the effluent.
- The model results can be used to determine whether discharge at the RIBs is functionally equivalent to a direct discharge to surface water. The following analysis is based on the DEQ guidance “Determining if a WPCF permit should be a NPDES permit under the Maui Supreme Court Decision” (DEQ, 2024b). Accordingly, seven factors are identified from which to base a determination of functional equivalency. The one-dimensional reactive transport geochemical model addresses two of these factors:
 - **Factor 4: the extent to which the pollutant is diluted or chemically changed as it travels.** DEQ guidance states that “(o)nce the effluent reaches groundwater, it can be diluted or chemically changed by the groundwater, aquifer material, or aquifer sediments” (DEQ, pg. 9, 2024b). The guidance does not establish thresholds for evaluating the extent of pollutant dilution. However, the guidance states that “. . . the permit writer, in consult with a DEQ hydrogeologist, should consider the extent to which the pollutants in question are diluted or chemically changed as they travel, however this factor will not, on its own, support a finding of a functional equivalent of a direct discharge” (DEQ, pg. 9, 2024b).
 - The Piper Diagram and Radar Diagram show that flow through and interaction with the aquifer solids alters the signature of the wastewater effluent by the time it reaches the Santiam River.
 - Parameters like pH and TDS are lower than values observed in wastewater effluent, reflecting the changes due to dilution and interactions with aquifer solids.
 - Parameters like TSS and BOD are also expected to have significant decreases over the flow path, as reduced forms of nitrogen and carbon are expected to be consumed by available oxygen in the groundwater, in addition to physical filtration of the suspended particles (i.e., TSS).
 - **Factor 7: the degree to which the pollution (at that point) has maintained its specific identity.** DEQ guidance states that “(f)actor 7 considers all the pollutants from the effluent in aggregate and requires a determination of how close the discharge into the navigable

water is in composition to the original effluent from the point source.” The guidance does not establish thresholds for evaluating the degree to which pollutants have maintained their specific identity. The guidance states that “(t)he permit writer will want to consider all the relevant pollutants that are part of the effluent and therefore will want data fully characterizing the effluent, groundwater, discharge at the navigable water, and ambient for those pollutants. Once this data(sic) is in hand then the permit writer can determine which pollutants are found in the discharge to the navigable water and how much they have changed using a Piper Diagram or other graphing technique. Consult with a DEQ hydrologist to determine the degree to which a pollutant maintains its identity.”

- The pH in wastewater effluent-influenced water will be similar to the background range by the time it arrives at the Santiam River.
- The TDS concentration in effluent-influenced water will decrease from that introduced by the wastewater effluent at the RIBs. TDS composition will undergo a chemical transformation, predominantly in terms of minor amounts of mineral precipitation and substitution of the effluent sodium for calcium associated with the aquifer solids.
- Ammonia will oxidize to nitrate along the flow path, consuming BOD and altering the pollutant identity accordingly.

9.0 Closing

We appreciate the opportunity to continue work with GSI on the Geochemical Assessment to support evaluation of treated wastewater infiltration in Gates and Mill City, Oregon. Please do not hesitate to contact us with respect to this technical memorandum.



Shannon Zahuranec PG
Senior Geochemist



Gregory Lehn, PhD
Senior Geochemist



James Jonas, PhD
Geochemist, Principal Consultant

10.0 References

- Bradford, S. A., Simunek, J., Bettahar, M., van Genuchten, M. T., & Yates, S. R. (2006). Significance of straining in colloid deposition: Evidence and implications. *Water Resources Research*, 42(12), W12S15.
- Cravotta, C.A. III, 2020. Interactive PHREEQ-N-AMDTreat water-quality modeling tools to evaluate performance and design of treatment systems for acid mine drainage (software download). U.S. Geological Survey Software Release. <https://doi.org/10.5066/P9QEE3D5>.
- Dzombak, D.A. and Morel, F.M., 1991. Surface complexation modeling: hydrous ferric oxide. John Wiley & Sons.
- DEQ. 2024b. Determining if a WPCF permit should be a NPDES permit under the Maui Supreme Court Decision. <https://www.oregon.gov/deq/wq/Documents/wqp-161-GUIDE-IMDDirectDischarge.pdf>.
- GSI Water Solutions Inc. (GSI). 2024a. Water Quality Sampling and Analysis to Support the Evaluation of Treated Wastewater Infiltration in Gates and Mill City, Marion and Linn Counties, Oregon. August 27.
- GSI. 2024b. Groundwater Level Monitoring to Support and Evaluation of Treated Wastewater Infiltration in Gates and Mill City, September 2023 to April 2024.
- GSI. 2024c. Evaluation of the Environmental Fate of Residual Nitrate from an Advance (Class A) Treated Wastewater Infiltration System, Mill City, Oregon. November 26.
- GSI. 2023a. Evaluation of the Environmental Fate of Residual Pollutants from an Advance (Class A) Treated Wastewater Infiltration System, Mill City, Oregon. November 16.
- GSI. 2023b. Phase II Subsurface Characterization to Support an Evaluation of Treated Wastewater Infiltration in Gates and Mill City, Marion and Linn Counties, Oregon. September 12.
- GSI. 2023c. Gates/Mill City Shallow Soil Characterization and Infiltration Testing Results, Marion and Linn Counties. Oregon. June 23.
- GSI. 2023d. Phase III Subsurface Characterization to Support an Evaluation of Treated Wastewater Infiltration in Gates and Mill City, Marion and Linn Counties, Oregon. November 15.
- GSI. In press. Infiltration Basin Pilot Test to Support an Evaluation of Treated Wastewater Infiltration in Gates and Mill City, Marion and Linn Counties, Oregon.
- Karamalidis, A.K. and Dzombak, D.A., 2010. Surface complexation modeling: gibbsite. John Wiley & Sons.
- Keller Associates (Keller), 2024a. Preliminary Engineering Report - Volume 1. City of Mill City. Water Pollution Control Facility Predesign. Prepared For Marion County, Oregon. September 30, 2024.
- Keller. 2024b. Draft Preliminary Engineering Report: Phase 2 Mill City/Gates Wastewater System.
- National Atmospheric Deposition Program (NRSP-3). 2022. NADP Program Office, Wisconsin State Laboratory of Hygiene, 465 Henry Mall, Madison, WI 53706.
- Oregon Department of Environmental Quality (DEQ). 2024a. Email from Mary Camarata (DEQ) to Chris Einmo (Marion County) RE: DEQ Comments on the Groundwater Model Report. January 16.

- Parkhurst, D.L. and Appelo, C.A.J., 2013. Description of input and examples for PHREEQC version 3: a computer program for speciation, batch-reaction, one-dimensional transport, and inverse geochemical calculations (No. 6-A43). United States Geological Survey.
- Smith, K.S. and Huyck, H.L.O. 1999. Abundance, relative mobility, bioavailability, and human toxicity of metals. - In Plumlee, G.S. & Logsdon, M.J. (eds): The environmental geochemistry of mineral deposits. Rev. in Economic Geol. 6: 29-70.
- Tessier, A.P.G.C., Campbell, P.C. and Bisson, M.J.A.C., 1979. Sequential extraction procedure for the speciation of particulate trace metals. Analytical chemistry, 51(7), pp.844-851.
- Tonkin, J.W., Balistrieri, L.S. and Murray, J.W., 2004. Modeling sorption of divalent metal cations on hydrous manganese oxide using the diffuse double layer model. Applied Geochemistry, 19(1), pp.29-53.
- United States Environmental Protection Agency (USEPA), 1998. MINTEQA2/PRODEFA2, A geochemical assessment model for environmental systems—User manual supplement for version 4.0: Athens, Georgia, National Exposure Research Laboratory, Ecosystems Research Division, 76 p. Revised September 2006.

Tables

Table 5-1: Acid Base Accounting and Total Metals Results for Aquifer Solids

Constituent	Units	Above the Water Table			At or Below the Water Table				
		GM1-MW4 6-8 ft	GM1-MW4 9-10 ft	GM1-MW4 10-11 ft	GM1-MW4 13-15 ft	GM1-MW4 16-20 ft	GM1-MW4 20-23 ft	GM1-MW4 25-26 ft	GM1-MW4 29-30 ft
Acid Base Accounting									
Solids, Percent	%	77.8	78.4	78.7	90.2	93.7	91.6	94.1	90.5
Sulfur Total	%	<0.1	<0.1	<0.1	<0.1	<0.1	<0.1	<0.1	<0.1
Sulfur Pyritic Sulfide	%	<0.1	<0.1	<0.1	<0.1	<0.1	<0.1	<0.1	<0.1
Sulfur Sulfate	%	<0.1	<0.1	<0.1	<0.1	<0.1	<0.1	<0.1	<0.1
Acid Generation Potential (calc on Sulfur total)	tCaCO ₃ /kt	<3.1	<3.1	<3.1	<3.1	<3.1	<3.1	<3.1	<3.1
Acid Neutralization Potential (calc)	tCaCO ₃ /kt	11	10	9	26	16	14	14	12
Net Neutralization Potential	tCaCO ₃ /kt	11	10	9	26	16	14	14	12
pH, Saturated Paste	units	5.8	5.9	6.6	7.9	7.6	7.8	8.3	8.2
Total Metals									
Aluminum	mg/kg	40,700	35,000	33,200	22,000	22,800	24,400	22,600	22,300
Antimony	mg/kg	<1.04	<1.03	<1.04	<1	<1.01	<1.01	<1.01	<1.01
Arsenic	mg/kg	4.0	3.9	7.9	3.9	2.2	3.0	2.6	3.1
Barium	mg/kg	151	116	113	65	54	55	39	58
Beryllium	mg/kg	0.69	0.71	0.65	0.53	0.36	0.39	0.34	0.29
Boron	mg/kg	3.3	3.5	3.7	4.1	3.4	3.5	<10.1	<10.1
Cadmium	mg/kg	0.95	1.0	0.97	0.83	0.76	0.72	0.69	0.47
Calcium	mg/kg	7,010	7,330	7,790	12,800	10,800	13,800	13,500	10,600
Chromium	mg/kg	31	32	22	20	17	22	16	13
Copper	mg/kg	32	36	34	37	29	43	30	26
Iron	mg/kg	36,800	32,200	35,100	27,900	26,300	25,000	21,800	25,500
Lead	mg/kg	5.0	5.3	4.4	4.5	3.0	2.7	3.7	2.8
Lithium	mg/kg	12	10	10	9.0	8.5	7.6	7.7	8.7
Magnesium	mg/kg	8,820	7,240	6,980	8,410	8,070	7,180	6,120	7,120
Manganese	mg/kg	697	511	621	718	445	453	257	308
Mercury by Direct Combustion AA	µg/kg	31	61	20	152	13	7.4	25	19
Molybdenum	mg/kg	<10.4	<10.3	<10.4	<10	<10.1	<10.1	<10.1	<10.1
Nickel	mg/kg	37	33	32	22	23	28	19	19
Phosphorus	mg/kg	464	381	740	823	783	824	773	722
Potassium	mg/kg	948	703	967	862	967	785	751	1,060
Selenium	mg/kg	0.095	0.11	0.079	0.051	<0.126	<0.126	<0.126	0.054
Silver	mg/kg	0.18	0.17	0.16	0.12	0.12	0.12	0.11	0.073
Sodium	mg/kg	932	1,120	1,350	2,200	2,420	3,020	2,990	2,540
Strontium	mg/kg	137	132	132	160	120	139	134	125
Thallium	mg/kg	0.090	0.099	0.13	0.058	<0.253	<0.253	<0.253	<0.253
Uranium	mg/kg	0.61	0.66	0.55	0.55	0.37	0.37	0.45	0.35
Vanadium	mg/kg	106	133	130	128	85	122	107	93
Zinc	mg/kg	66	56	58	51	49	43	39	41

Notes: % - percent; t CaCO₃/kt - tons of calcium carbonate per ton of material; meq/100g - milliequivalents per 100 grams; ft - feet; mg/kg - milligrams per kilogram; µg/kg - micrograms per kilogram; < - less than

Table 5-2: Mineralogical Composition and Cation Exchange Capacity for Aquifer Solids

Mineral	Mineral Formula	Above the Water Table			At or Below the Water Table				
		GM1-MW4 6-8 ft	GM1-MW4 9-10 ft	GM1-MW4 10-11 ft	GM1-MW4 13-15 ft	GM1-MW4 16-20 ft	GM1-MW4 20-23 ft	GM1-MW4 25-26 ft	GM1-MW4 29-30 ft
Mineralogy (wt %)									
Quartz	SiO ₂	11	8	10	13	13	9	10	15
Tridymite	SiO ₂	0	0	0	0	3	0	0	0
Plagioclase	NaAlSi ₃ O ₈	32	34	39	44	42	45	45	51
Pyroxene	XY(Si,Al) ₂ O ₆	4	4	5	6	5	9	7	5
Chlorite	(Fe, ^(Mg,Mn) 5,Al) (Si ₃ Al)O ₁₀ (OH) ₈	0	0	0	2	2	1	1	3
Smectite	(Na,Ca) _{0.33} (Al,Mg) ₂ (Si ₄ O ₁₀)(OH) ₂ ·nH ₂ O	52	53	45	35	34	36	37	26
Hematite	Fe ₂ O ₃	1	1	1	0	1	0	0	0
Cation Exchange Capacity (meq/100g)									
CEC	--	22.3	22.3	17.7	7.9	7.3	7.1	6.3	5.6

Table 5-3: Sequential Extraction Procedure Results for Aquifer Solids

Constituent or SEP Step	Units	Above the Water Table		At or Below the Water Table	
		GM1-MW4 6-8 ft	GM1-MW4 9-10 ft	GM1-MW4 20-23 ft	GM1-MW4 25-26 ft
Iron					
SEP Step 1: Exchangeable Fraction	mg/kg	46	61	99	107
SEP Step 2: Carbonate Fraction	mg/kg	0	0	0	10
SEP Step 3: Non-Crystalline Minerals Fraction	mg/kg	15	21	274	301
SEP Step 4: Metal Hydroxide Fraction	mg/kg	3,640	4,720	2,460	1,552
SEP Step 5: Organic and Sulfide Fraction	mg/kg	204	282	36	24
SEP Step 6: Residual Fraction	mg/kg	33,500	29,900	24,900	21,700
Sum of SEP Steps 1-6	mg/kg	37,405	34,984	27,769	23,694
Total Digestion	mg/kg	36,800	32,200	25,000	21,800
RPD between Sum of SEP Steps and Total Digestion	%	2	8	10	8
Aluminum					
SEP Step 1: Exchangeable Fraction	mg/kg	63	48	100	113
SEP Step 2: Carbonate Fraction	mg/kg	12	9	13	17
SEP Step 3: Non-Crystalline Minerals Fraction	mg/kg	41	26	295	257
SEP Step 4: Metal Hydroxide Fraction	mg/kg	71	93	65	89
SEP Step 5: Organic and Sulfide Fraction	mg/kg	1,624	1,534	774	732
SEP Step 6: Residual Fraction	mg/kg	38,600	33,500	23,900	22,100
Sum of SEP Steps 1-6	mg/kg	40,410	35,209	25,147	23,308
Total Digestion	mg/kg	40,700	35,000	24,400	22,600
RPD between Sum of SEP Steps to Total Digestion	%	-1	1	3	3
Manganese					
SEP Step 1: Exchangeable Fraction	mg/kg	1	1	4	2
SEP Step 2: Carbonate Fraction	mg/kg	6	6	16	4
SEP Step 3: Non-Crystalline Minerals Fraction	mg/kg	4	6	70	14
SEP Step 4: Metal Hydroxide Fraction	mg/kg	262	204	123	24
SEP Step 5: Organic and Sulfide Fraction	mg/kg	195	120	25	7
SEP Step 6: Residual Fraction	mg/kg	269	219	240	212
Sum of SEP Steps 1-6	mg/kg	737	556	477	262
Total Digestion	mg/kg	697	511	453	257
RPD between Sum of SEP Steps to Total Digestion	%	6	8	5	2

Notes: mg/kg - milligrams per kilogram; % - percent; SEP - sequential extraction procedure; ft - feet

Table 5-4: Water Quality Results for Groundwater at GM1 and Treatment Plant Influent

Constituent	Detection Limit	Units	Groundwater at GM1*			Treatment Plant Influent	
			GM1-MW1	GM1-MW2	GM1-MW4	IN_20230502	WW-050124
			5/28/23	4/25/24	4/25/24	5/2/23	5/1/24
Field pH		pH Units	6.5	6.5	6.3	--	--
Field Conductivity		µS/cm	93.3	255.0	252.0	--	--
Dissolved Oxygen		mg/L	6.0	3.5	3.3	--	--
ORP		mV	93.8	107.5	186.6	--	--
Temperature		°C	11.7	11.2	10.5	--	--
Turbidity		NTU	24.5	1.97	4.67	--	--
pH		pH Units	6.2	7.1	7.3	--	7.2
Conductivity	250	µmhos/cm	--	157	145	--	788
Total Dissolved Solids	5	mg/L	78	110	115	--	307
Total Suspended Solids	2	mg/L	11.5	--	--	--	--
Calcium	600	ug/L	10,500	17,700	15,400	--	21,500
Magnesium	150	µg/L	3,200	6,720	6,460	--	9,140
Sodium	100	µg/L	3,800	5,480	5,500	50,200	40,400
Potassium	100	µg/L	2,600	1,380	1,660	--	16,700
Sulfate	1	mg/L	1.60	2.05	2.06	--	10.9
Fluoride	1	mg/L	--	ND	ND	7.41	ND
Chloride	1	mg/L	1.40	1.92	1.84	--	37.1
Bromide	1	mg/L	--	ND	ND	--	ND
Total Alkalinity	20	mg CaCO ₃ /L	42.5	76.6	69	279	296
Bicarbonate Alkalinity	20	mg CaCO ₃ /L	42.5	76.6	69	340	296
Carbonate Alkalinity	20	mg CaCO ₃ /L	ND	ND	ND	--	ND
Hydroxide Alkalinity	20	mg CaCO ₃ /L	ND	ND	ND	--	ND
Ammonia as N	0.02	mg/L	--	ND	ND	--	51.8
Nitrate-Nitrogen as N	0.25	mg/L	1.10	0.308	0.699	ND	ND
Nitrite-Nitrogen as N	0.25	mg/L	ND	ND	ND	ND	ND
Phosphorus	0.2	mg/L	--	ND	ND	--	6.01
Total Cyanide	0.005	mg/L	ND	ND	ND	--	0.0235
Aluminum	50	µg/L	520	ND	139	275	189
Antimony	1	µg/L	ND	ND	ND	ND	ND
Arsenic	1	µg/L	ND	ND	ND	ND	1.02
Barium	2	µg/L	ND	2.13	2.98	10.9	9.83
Beryllium	0.2	µg/L	ND	ND	ND	ND	ND
Boron	10	µg/L	--	ND	ND	--	274
Cadmium	0.2	µg/L	ND	ND	ND	ND	ND
Chromium	2	µg/L	ND	ND	ND	ND	2.12
Copper	2	µg/L	2	ND	ND	ND	13.1
Iron	50	µg/L	620	--	--	286	0.792
Lead	0.2	µg/L	ND	ND	1.79	ND	--
Lithium	5	µg/L	--	ND	ND	--	ND
Manganese	1	µg/L	77.6	8.31	40.3	ND	28.7
Mercury	0.08	µg/L	ND	ND	ND	ND	ND
Molybdenum	1	µg/L	0.62	ND	ND	--	ND
Nickel	2	µg/L	0.86	ND	ND	ND	2.19
Selenium	1	µg/L	ND	ND	ND	ND	ND
Silica	50	µg/L	30000	--	--	--	--
Silver	0.2	µg/L	ND	ND	ND	ND	ND
Strontium	5	µg/L	--	93.4	86.4	--	94.9
Thallium	0.2	µg/L	ND	ND	ND	ND	ND
Vanadium	2	µg/L	--	2.09	3.56	--	4.09
Zinc	4	µg/L	3.30	ND	ND	54.7	61.5

Notes: ND - concentration below detection limit; -- - Not analyzed; µmhos/cm - microohms per centimeter; mg/L - milligrams per liter; µg/L - micrograms per liter; CaCO₃ - calcium carbonate; °C - degrees Celsius; NTU - nephelometric turbidity units.

* Results from samples GM1-MW4 and GM1-MW5 collected in 2023 are not included in this table, but can be found in GSI, 2024a.

Table 6-1: Water Quality Results for Groundwater at GM1-MW4 and Expected Treatment Plant Effluent

Constituent	Units	Base Case		
		Site Precipitation	Upgradient Groundwater	Treatment Plant Effluent
pH	S.U.	5.4	6.3	7.2
pe	unitless	--	6.5	6.0
Total Dissolved Solids	mg/L	0.82	115	226
Total Suspended Solids	mg/L	--	12	20
Calcium	mg/L	0.026	15	22
Magnesium	mg/L	0.020	6.5	9.1
Sodium	mg/L	0.17	5.5	40
Potassium	mg/L	0.011	1.7	17
Sulfate	mg/L	0.16	2.1	11
Fluoride	mg/L	--	0.50	ND
Chloride	mg/L	0.29	1.8	37
Total Alkalinity	mg CaCO ₃ /L	--	69	80
Ammonia as N	mg/L	0.020	0.010	1.0
Nitrate-Nitrogen as N	mg/L	0.12	0.50	1.0
Nitrite-Nitrogen as N	mg/L	--	0.13	0.13
Aluminum	mg/L	--	0.14	0.19
Antimony	mg/L	--	0.0005	0.0005
Arsenic	mg/L	--	0.0005	0.0010
Barium	mg/L	--	0.0030	0.0098
Beryllium	mg/L	--	0.00010	0.0001
Boron	mg/L	--	0.0050	0.27
Cadmium	mg/L	--	0.00010	0.0001
Chromium	mg/L	--	0.0010	0.0021
Copper	mg/L	--	0.0010	0.013
Iron	mg/L	--	0.62	0.00079
Lead	mg/L	--	0.0018	0.0001
Lithium	mg/L	--	0.0025	0.0025
Manganese	mg/L	--	0.040	0.029
Mercury	mg/L	--	0.000040	0.00004
Molybdenum	mg/L	--	0.00050	0.0005
Nickel	mg/L	--	0.0010	0.0022
Selenium	mg/L	--	0.00050	0.0005
Silver	mg/L	--	0.00010	0.0001
Strontium	mg/L	--	0.086	0.095
Thallium	mg/L	--	0.00010	0.0001
Vanadium	mg/L	--	0.0036	0.0041
Zinc	mg/L	--	0.0020	0.062

Notes:

Analytes measured below the detection limit were modeled at ½ the detection limit

Bold italicized values were modified off the original data source (GM1-MW4 or Plant Influent) based on the modifications outlined in Section 6.4.1.

-- value not measured; S.U. - standard units; mg/L - milligrams per liter; CaCO₃ - calcium carbonate; N - nitrogen.

Table 6-2: Conversion of Iron, Aluminum, and Manganese SEP Results to Initial Mineral Concentrations

Constituent	Assumed Mineral Form	Metal Atomic Mass	Average in Unsaturated Solids based on SEP Steps 3 and 4		Average in Saturated Solids based on SEP Steps 3 and 4	
		g/mol	mg/kg of soil	mol/L of water	mg/kg of soil	mol/L of water
Iron	Ferrihydrite	55.85	4,198	0.053	2,293	0.035
Aluminum	Gibbsite	26.982	115	0.0036	353	0.011
Manganese	Manganite	54.94	238	0.0037	115	0.0018

Note: The initial concentration of minerals was calculated using the following equation for conversion from mg of metal per kilogram of soil to moles of mineral per L of water:

$$\left(\frac{\text{mg of metal}}{\text{kg of sand/fines}}\right) * \left(\frac{0.2 \text{ kg of sand/fines}}{1.0 \text{ kg of bulk soil}}\right) * \left(\frac{\text{moles of metal}}{\text{g of metal}}\right) * \left(\frac{\text{moles of mineral}}{\text{moles of metal}}\right) * \left(\frac{\text{kg of bulk soil}}{\text{L of bulk soil}}\right) * \left(\frac{1}{\text{porosity}}\right) = \left(\frac{\text{moles of mineral}}{\text{L of water}}\right)$$

Table 6-3: Sorption Site Details for Iron, Aluminum, and Manganese Oxides

Constituent	Assumed Mineral Form	Specific Surface Area	Sorption Site Names	Surface Site Conc.	Surface Area
		m ² /g		mols of sites per mol of mineral	m ² /mol of mineral
Iron	Ferrihydrite	600	FeOH weak	0.20	53,300
			FeOH strong	0.005	53,300
Aluminum	Gibbsite	32	AlOH	0.033	2,496
Manganese	Manganite	746	MnOH_x	0.141	78,330
			MnOH_y	0.079	78,330

Table 7-1: Water Quality Modeled Results for Groundwater at Santiam River and Treatment Plant Effluent

Parameter	Units	Background Groundwater	Modeling Results																			
			Effluent-Base Case	GW at Santiam River (Year 5) Base Case	GW at Santiam River (Year 10) Base Case	GW at Santiam River (Year 20) Base Case	Effluent-Sensitivity #1 (Low pH)	GW at Santiam River (Year 5) Sensitivity #1	GW at Santiam River (Year 10) Sensitivity #1	GW at Santiam River (Year 20) Sensitivity #1	Effluent-Sensitivity #2 (High pH)	GW at Santiam River (Year 5) Sensitivity #2	GW at Santiam River (Year 10) Sensitivity #2	GW at Santiam River (Year 20) Sensitivity #2	Effluent-Sensitivity #3 (Higher RIB Flow)	GW at Santiam River (Year 5) Sensitivity #3	GW at Santiam River (Year 10) Sensitivity #3	GW at Santiam River (Year 20) Sensitivity #3	Effluent-Sensitivity #4 (Higher Nitrate)	GW at Santiam River (Year 5) Sensitivity #4	GW at Santiam River (Year 10) Sensitivity #4	GW at Santiam River (Year 20) Sensitivity #4
pH	S.U.	6.3	7.0	6.8	6.9	6.9	6.5	6.7	6.8	6.8	8.5	6.9	7.0	7.0	7.0	6.8	6.9	6.9	7.0	6.9	7.0	7.0
Total Dissolved Solids	mg/L	110	223	203	206	206	216	193	195	195	248	216	219	219	223	206	209	209	223	237	240	240
Calcium	mg/L	15	22	32	31	31	22	31	30	30	22	32	31	31	22	32	31	31	22	36	35	35
Magnesium	mg/L	6.5	9.1	13	13	13	9.1	13	12	12	9.1	13	13	13	9.1	13	13	13	9.1	15	14	14
Sodium	mg/L	5.5	40	24	24	24	40	24	24	24	48	28	29	29	40	25	25	25	40	25	25	25
Potassium	mg/L	1.7	17	2.3	5.2	5.2	17	2.3	5.0	5.0	17	2.3	5.3	5.3	17	2.3	5.3	5.3	17	2.5	5.5	5.5
Sulfate	mg/L	2.1	11	10	10	10	11	9.8	9.8	9.8	11	10	10	10	11	10	10	10	11	9.7	9.6	9.6
Fluoride	mg/L	0.50	0.50	0.75	0.74	0.74	0.50	0.71	0.69	0.69	0.50	0.78	0.76	0.76	0.50	0.77	0.74	0.74	0.50	0.58	0.55	0.55
Chloride	mg/L	1.8	39	29	29	29	55	40	40	40	37	27	27	27	39	30	30	30	36	26	26	26
Alkalinity	mg CaCO ₃ /L	69	74	83	84	84	52	64	65	65	94	94	95	95	74	84	85	85	74	110	111	111
Ammonia as N	mg/L	0.010	1.0	0	0	0	1.0	0	0	0	1.0	0	0	0	1.0	0	0	0	1.0	0	0	0
Nitrate-Nitrogen	mg/L	0.56	1.0	1.7	1.7	1.7	1.0	1.7	1.7	1.7	1.0	1.7	1.7	1.7	1.0	1.7	1.7	1.7	5.0	4.6	4.6	4.6
Nitrite-Nitrogen	mg/L	0.13	0.13	2.1E-13	2.1E-13	2.1E-13	0.13	2.1E-13	2.1E-13	2.1E-13	0.13	2.1E-13	2.1E-13	2.1E-13	0.13	2.2E-13	2.1E-13	2.1E-13	0.13	5.7E-13	5.7E-13	5.7E-13
Aluminum	mg/L	0.14	0.14	0.19	0.0012	0.0011	0.0011	0.19	0.0016	0.0013	0.0013	0.19	0.0012	0.0011	0.0011	0.19	0.0013	0.0011	0.0011	0.19	0.00099	0.00097
Antimony	mg/L	0.00050	0.00050	0.00050	0.00049	0.00049	0.00049	0.00050	0.00049	0.00049	0.00049	0.00050	0.00049	0.00049	0.00049	0.00050	0.00049	0.00049	0.00049	0.00050	0.00049	0.00049
Arsenic	mg/L	0.00050	0.00050	0.0010	0.00087	0.00087	0.00087	0.0010	0.00087	0.00087	0.00087	0.0010	0.00087	0.00087	0.00087	0.0010	0.00088	0.00088	0.00088	0.0010	0.00087	0.00087
Barium	mg/L	0.0030	0.0030	0.0098	0.0055	0.0054	0.0054	0.0098	0.0053	0.0052	0.0052	0.0098	0.0055	0.0054	0.0054	0.0098	0.0056	0.0055	0.0055	0.0098	0.0063	0.0062
Beryllium	mg/L	0.00010	0.00010	0.00010	0.00010	0.00010	0.00010	0.00010	0.00010	0.00010	0.00010	0.00010	0.00010	0.00010	0.00010	0.00010	0.00010	0.00010	0.00010	0.00010	0.00010	0.00010
Boron	mg/L	0.0050	0.0050	0.27	0.20	0.20	0.20	0.27	0.20	0.20	0.20	0.27	0.20	0.20	0.20	0.27	0.20	0.20	0.20	0.27	0.20	0.20
Cadmium	mg/L	0.00010	0.00010	0.00010	0.00016	0.00015	0.00015	0.00010	0.00019	0.00017	0.00017	0.00010	0.00016	0.00014	0.00014	0.00010	0.00017	0.00014	0.00014	0.00010	0.00015	0.00013
Chromium	mg/L	0.0010	0.0010	0.0021	0.0018	0.0018	0.0018	0.0021	0.0018	0.0018	0.0018	0.0021	0.0018	0.0018	0.0018	0.0021	0.0018	0.0018	0.0018	0.0021	0.0018	0.0018
Copper	mg/L	0.0010	0.0010	0.013	0.00003	0.00003	0.00003	0.013	0.00003	0.00002	0.00002	0.013	0.00003	0.00003	0.00003	0.013	0.00003	0.00003	0.00003	0.013	0.00004	0.00003
Iron	mg/L	0.62	0.62	0.00079	0.00091	0.00082	0.00082	0.00079	0.0012	0.0011	0.0011	0.00079	0.00087	0.00073	0.00073	0.00079	0.00096	0.00078	0.00078	0.00079	0.00077	0.00063
Lead	mg/L	0.0018	0.0018	0.00010	0.00003	0.00003	0.00003	0.00010	0.00003	0.00002	0.00002	0.00010	0.00003	0.00003	0.00003	0.00010	0.00003	0.00003	0.00003	0.00010	0.00003	0.00003
Lithium	mg/L	0.0025	0.0025	0.0025	0.0030	0.0030	0.0030	0.0025	0.0030	0.0030	0.0030	0.0025	0.0031	0.0031	0.0031	0.0025	0.0030	0.0030	0.0030	0.0025	0.0031	0.0031
Manganese	mg/L	0.040	0.040	0.029	0.00002	0.00001	0.00001	0.029	0.00003	0.00002	0.00002	0.029	0.00001	0.00001	0.00001	0.029	0.00002	0.00001	0.00001	0.029	0.00001	0.00001
Mercury	mg/L	0.00004	0.00004	0.00004	0.00004	0.00004	0.00004	0.00004	0.00004	0.00004	0.00004	0.00004	0.00004	0.00004	0.00004	0.00004	0.00004	0.00004	0.00004	0.00004	0.00004	0.00004
Molybdenum	mg/L	0.00050	0.00050	0.00050	0.00049	0.00049	0.00049	0.00050	0.00049	0.00049	0.00049	0.00050	0.00049	0.00049	0.00049	0.00050	0.00049	0.00049	0.00049	0.00050	0.00049	0.00049
Nickel	mg/L	0.0010	0.0010	0.0022	0.0018	0.0018	0.0018	0.0022	0.0018	0.0018	0.0018	0.0022	0.0018	0.0018	0.0018	0.0022	0.0019	0.0019	0.0019	0.0022	0.0018	0.0018
Selenium	mg/L	0.00050	0.00050	0.00050	0.00049	0.00049	0.00049	0.00050	0.00049	0.00049	0.00049	0.00050	0.00049	0.00049	0.00049	0.00050	0.00049	0.00049	0.00049	0.00050	0.00049	0.00049
Silver	mg/L	0.00010	0.00010	0.00010	0.00010	0.00010	0.00010	0.00010	0.00010	0.00010	0.00010	0.00010	0.00010	0.00010	0.00010	0.00010	0.00010	0.00010	0.00010	0.00010	0.00010	0.00010
Strontium	mg/L	0.086	0.086	0.095	0.16	0.16	0.16	0.095	0.16	0.15	0.15	0.095	0.16	0.16	0.16	0.095	0.16	0.16	0.16	0.095	0.18	0.18
Thallium	mg/L	0.00010	0.00010	0.00010	0.00010	0.00010	0.00010	0.00010	0.00010	0.00010	0.00010	0.00010	0.00010	0.00010	0.00010	0.00010	0.00010	0.00010	0.00010	0.00010	0.00010	0.00010
Vanadium	mg/L	0.0036	0.0036	0.0041	0.0039	0.0039	0.0039	0.0041	0.0039	0.0039	0.0039	0.0041	0.0039	0.0039	0.0039	0.0041	0.0039	0.0039	0.0039	0.0041	0.0039	0.0039
Zinc	mg/L	0.0020	0.0020	0.062	0.00019	0.00018	0.00018	0.062	0.00022	0.00020	0.00020	0.062	0.00019	0.00017	0.00017	0.062	0.00020	0.00018	0.00018	0.062	0.00020	0.00017

Notes: Total Suspended Solids (TSS) could not be simulated in PHREEQC because the model does not simulate the settling and filtering of solids in the RIB and aquifer solids.
 S.U. - standard units; mg/L - milligrams per liter; CaCO₃ - calcium carbonate; GW - groundwater

Figures

Figure 4-1. Site GM1 Location (from GSI 2024a).

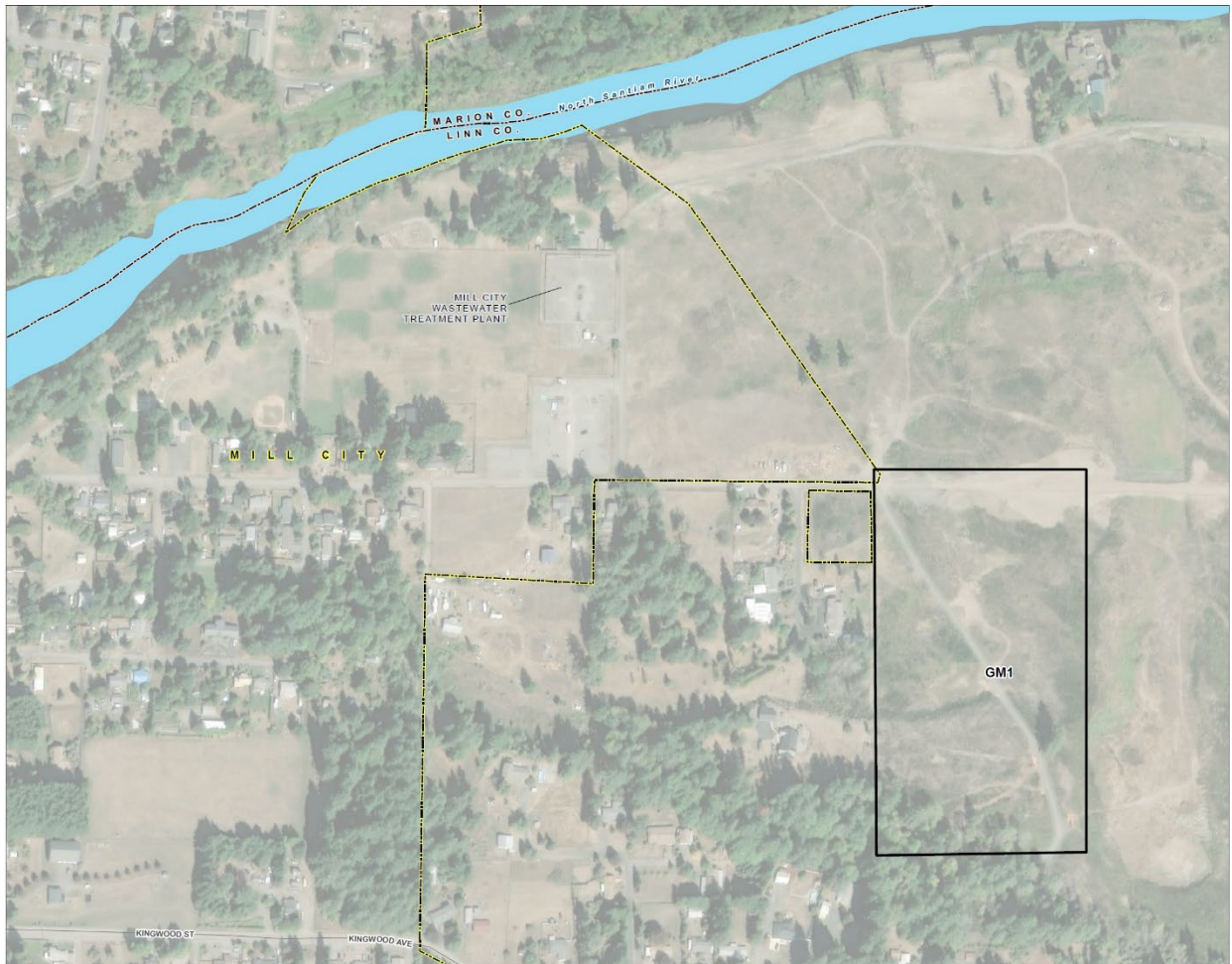
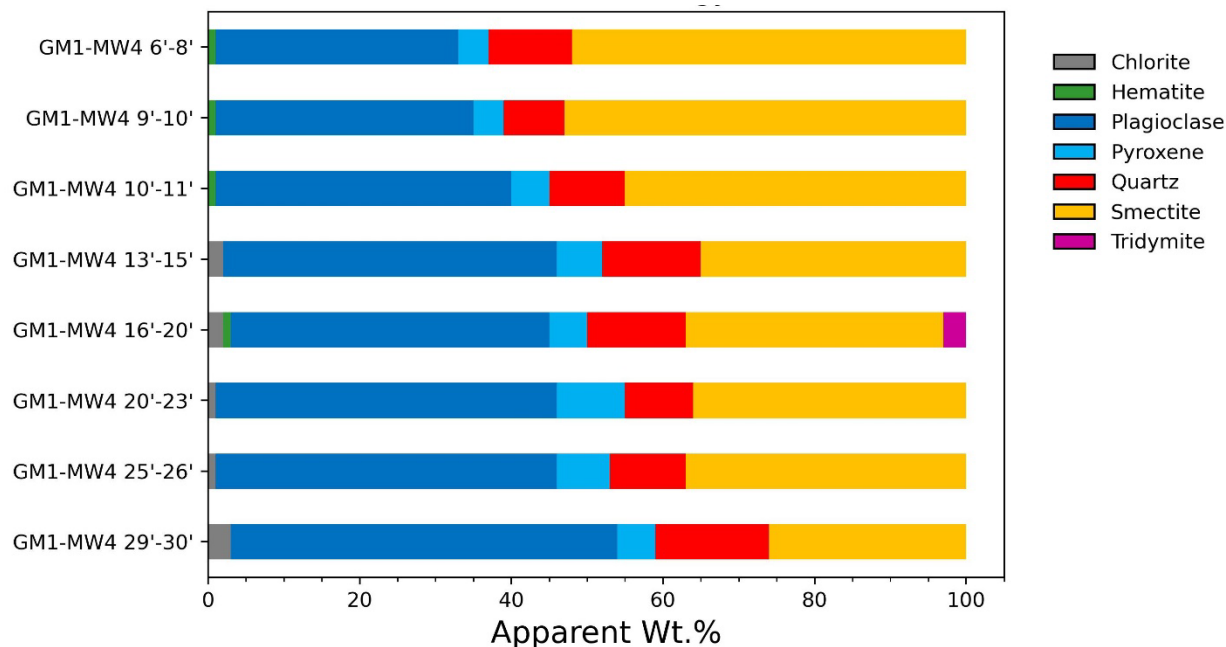


Figure 5-1. Monitoring Well Location Map (from GSI 2024a).



Figure 5-2: Mineralogical Composition of Soil Samples



Note: The proportion of clay (smectite) presented in this mineralogical composition is greater than measured in the field because it represents a weight percent of only the fine fraction, not including the gravel that was screened out prior to analysis by x-ray diffraction (XRD). Proportions of other minerals may be similarly affected by the sample screening.

Figure 5-3: Iron, Aluminum, and Manganese Concentrations in Sequential Extraction Procedure Fractions within GM1-MW4 Soil Samples

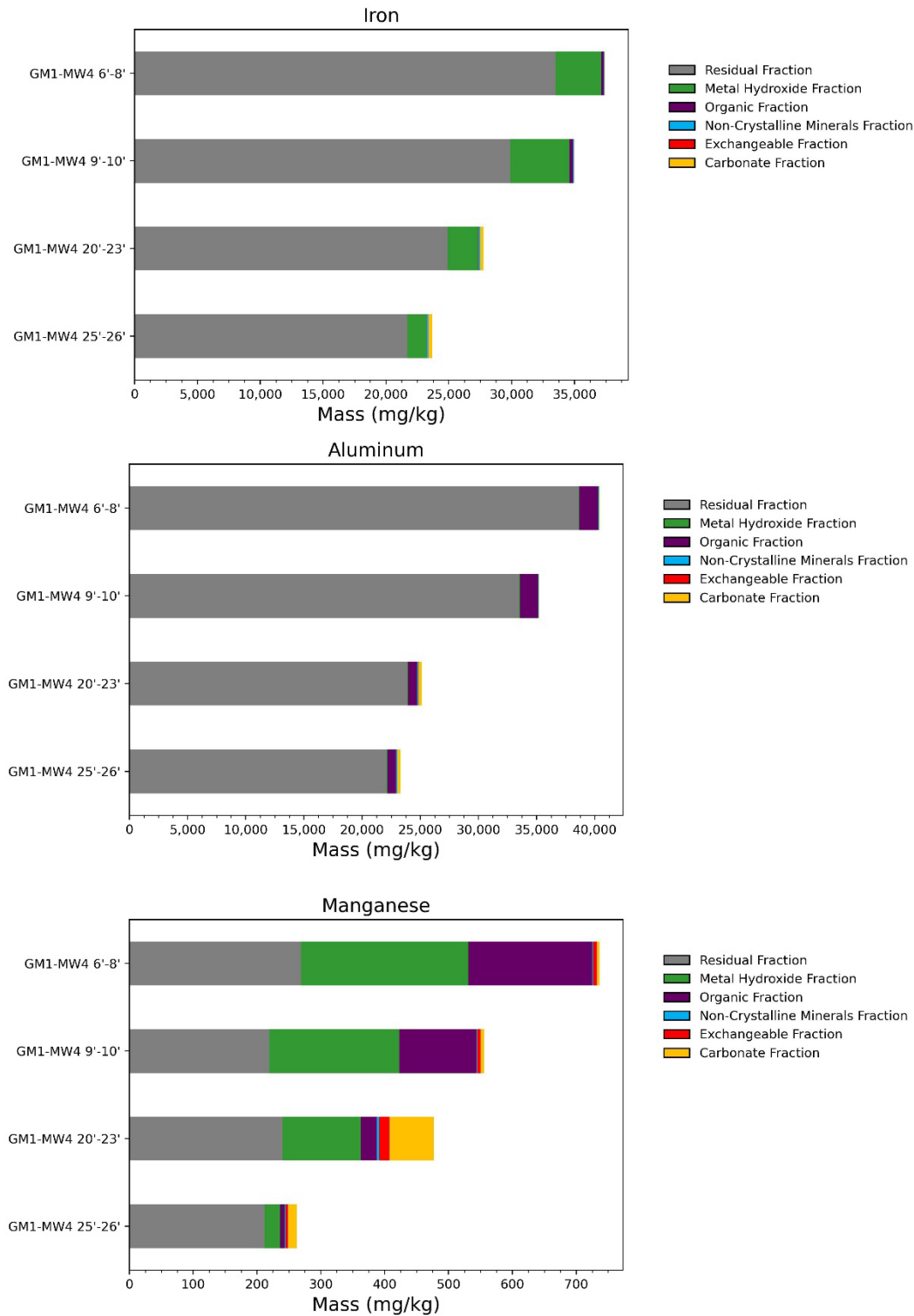


Figure 7-1: Piper Diagram of Modeled Groundwater Quality Predictions

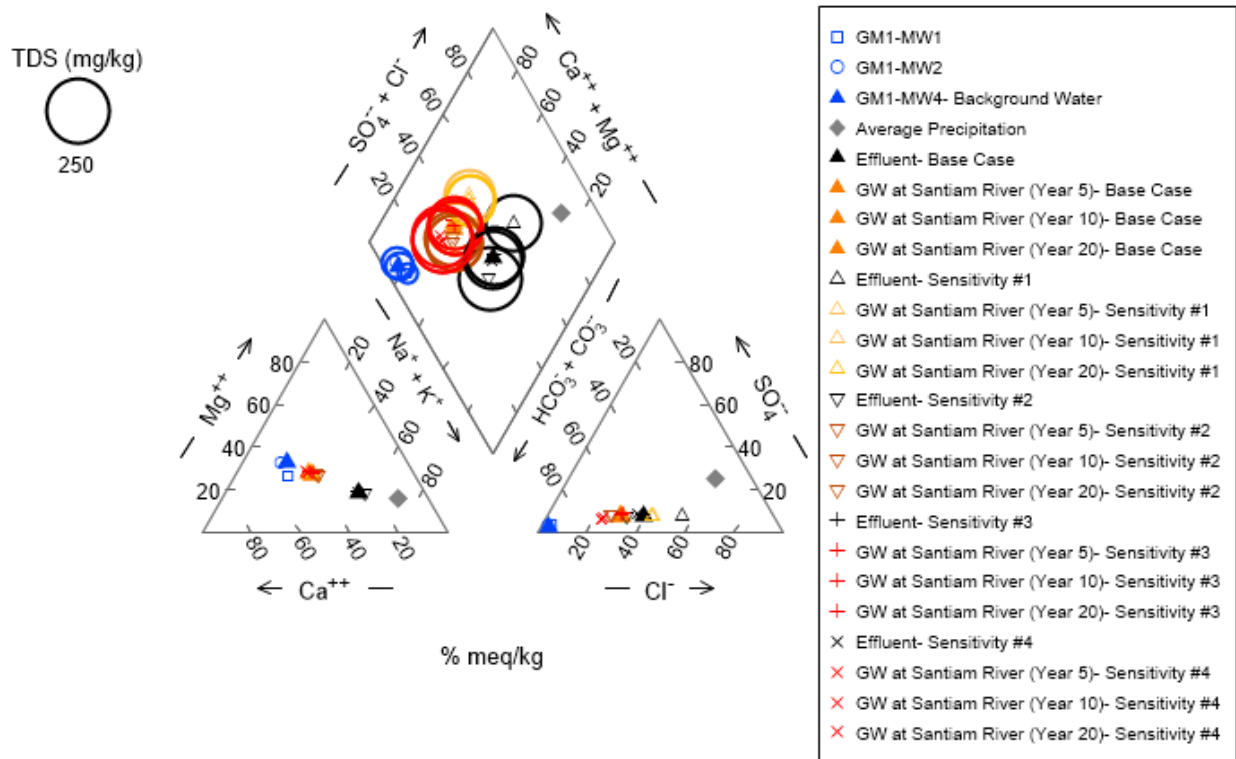


Figure 7-2: Selected trace metal concentrations in initial solutions and predicted water qualities

